5
Graphene as a counter electrode materials for high photo conversion efficiency

5.1 INVESTIGATION OF CHEMICALLY SYNTHESIZED GRAPHENE AS COUNTER ELECTRODE FOR DSSC

The counter electrode of the DSSC plays a key role in regenerating the electrolyte redox system. Mostly platinum is used as a standard counter electrode in DSSCs, it exhibits excellent chemical stability, high catalytic activity towards iodide-triiodide based electrolyte and more importantly high conductivity. However, the noble Pt is expensive metal which remarkably increases the cost of solar cell and confines its application as solar cell. The DSSC as a potential candidate to replace conventional solar cells, extensive research has been performed to find out suitable substitute for the precious platinum metal as a counter electrode material. Researchers have tried several functional materials like CoS, conducting polymers, nitrides and inorganic oxides to act as counter electrode in DSSC [Wang, *et al.*, 2009; Wu, *et al.*, 2011; Wu, *et al.*, 2012; Xu, *et al.*, 2012; Cho, *et al.*, 2012]. For efficient counter electrode, materials should fulfill few basic requirements like high catalytic activity towards iodide- triiodide based electrolyte, large specific surface area, chemical stability, low cast and high conductivity.

Recently, carbon materials such as graphite, carbon nanotubes, activated carbon, and graphene have been explored as very promising material for counter electrode [Liu, *et al.*, 2012; Hsieh, *et al.*, 2012]. Graphene, carbon atoms arranged in single layer hexagonal lattice has emerged as a potential candidate for counter electrode due to its excellent physical and electrical properties. Apart from fulfilling basic requirements required to act as counter electrode in DSSC, graphene also has been reported with optical transparency, robustness, stiffness, impermeable to gasses, high hole transport mobility and the inertness against oxygen and water vapor [Li, *et al.*, 2009]. Graphene has been formed by various techniques where few are prominent for good quality which includes micromechanical cleavage [Huang, *et al.*, 2009], electrochemically reduction of graphene oxide (GO) [Lee, *et al.*, 2008], thermal exfoliation from graphite oxide [Chou, *et al.*, 2015], the oxidative exfoliation of graphite by hydrazine reduction [Greijer, *et al.*, 2001], the chemical reduction of graphene oxide colloids under microwave irradiation [Smestad, *et al.*, 1994] and electrophoretic deposition with thermal treatment [Wang, *et al.*, 2008].

5.1.1 Synthesis and optimization of graphene counter electrode films

Graphene was synthesized by the Hummer's method from natural graphite, wherein graphene oxide has been reduced by the hydrazine hydrate treatment [Kaniyoor and Ramaprabhu, 2011]. To understand the nature of graphene counter electrode several fabrication methods have been explored in this work. Two different graphene-containing solutions were prepared and used for fabricating counter electrodes by three different methods - drop casting, spin coating and screen printing.

Suspension for the drop casting and spin coating were prepared with nafion:ethanol (1:1) and synthesized graphene. For drop casting, the above suspension was mounted on the

substrate using another glass slide, and then dried at room temperature as shown in Figure 5.1a. In spin coating, the above suspension was spin coated on the substrate (see Figure 5.1b). The synthesized graphene with terpienol solution contains 0.25% ethyl cellulose was used as a suspension to prepared counter electrode by screen printing and the detail process is explained in Figure 5.1c [Lim, *et al.*, 2013]. Then prepared suspensions were deposited on the substrate by screen printing. Films deposited by these three methods were annealed at different temperatures ranging from 250 to 400˚C.

The active electrode is made up of wideband semiconductor like titanium dioxide. In short, firstly TiO_2 (P25, Degussa) powder and n-butanol were vigorously mixed. The second solution was prepared by mixing deionized water and TiO_2 powder. Then the third solution was prepared by mixing ethyl cellulose and n-butanol. These solutions were vigorously stirred for 24 hours. Then, all the solutions were mixed together and kept at stirring for another 24 hours. Finally, poly (ethylene glycol) and terpineol were added. At last, the slurry was stirred for 24 hours. The active electrodes were fabricated using this TiO_2 viscous paste on FTO glass by screen printing technique (as described in Figure 5.1c).

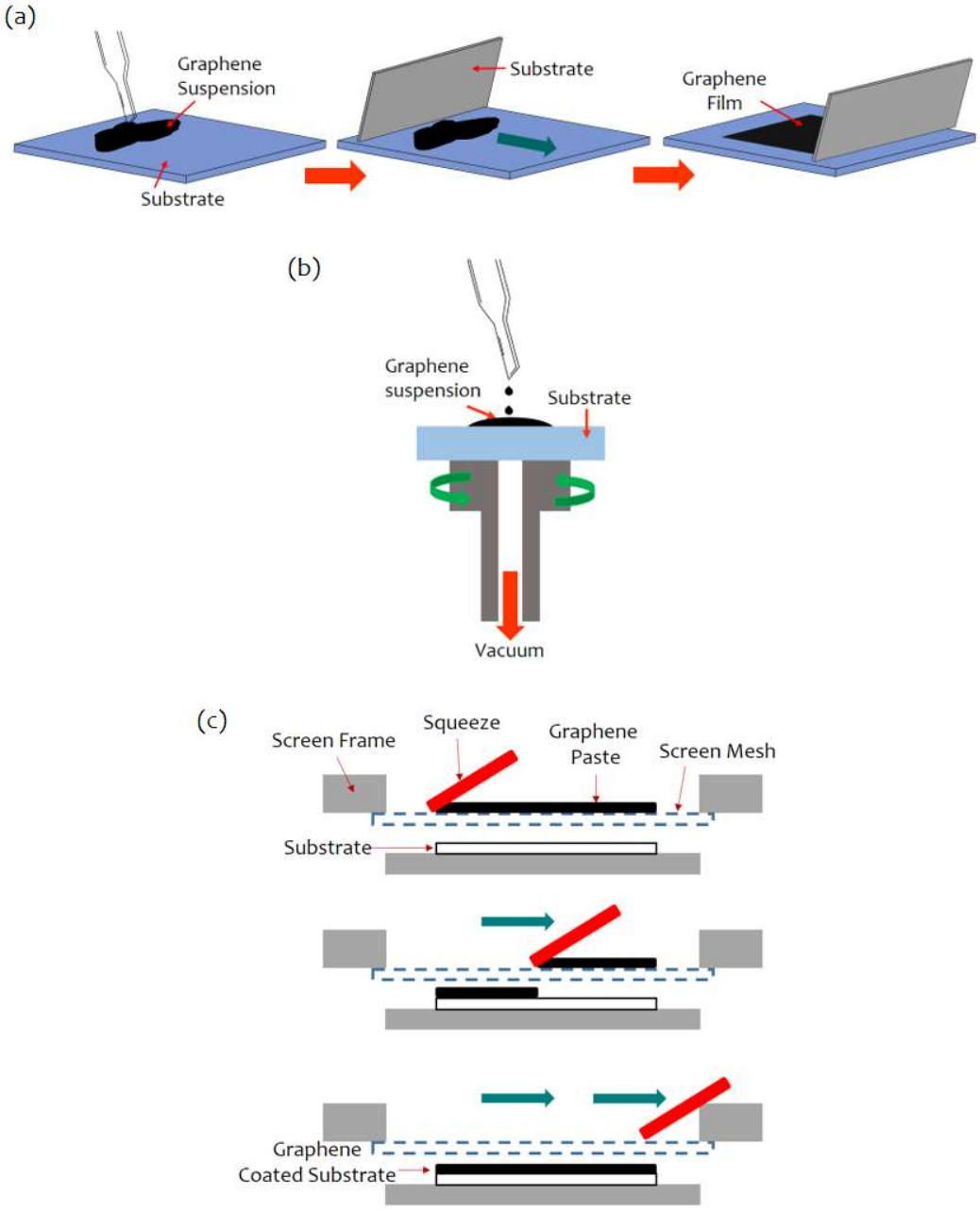

Figure 5.1 : Schematic illustration of (a) drop casting, (b) spin coating and (c) screen printing techniques

Before the fabrication, the conducting glass (FTO) was ultrasonically cleaned with deionized water, ethanol and acetone for 30 minutes each. The screen-printed TiO_2 films dried in a clean box at room temperature. Then photoanode films were annealed at 500˚C for 1 hour. The photoanode film was observed as 11µm thick. Then TiO_2 active electrodes were sensitized by immersing them into a 0.5 mM N719 dye solution ((1:1) tertbutyl alcohol and acetonitrile). The dye sensitized solar cells, TiO_2 working electrode and graphene counter-electrode were sandwiched together with the help of paper clamps. In clamped electrodes, a drop of electrolyte solution (Soloronix Iodolyte) was introduced.

5.1.2 Structural and morphological analysis of graphene

The transformation of graphite to graphene was examined by X-ray diffraction patterns as shown in Figure 5.2. In the conversion of graphite to graphene, the crystalline nature of graphite is destroyed. The intense peak at 26.5° in the diffraction pattern of graphite corresponds to the (002) plane and has d spacing of 3.36 Å.

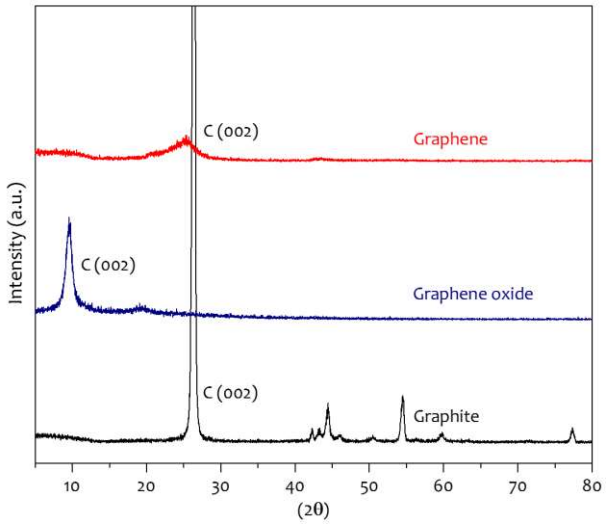

Figure 5.2 : XRD pattern of graphite, graphene oxide and graphene

This high-intensity characteristic peak of graphite confirms its highly crystalline nature. In the first step of graphene formation, graphite was reduced to graphene oxide and was confirmed using diffraction pattern. The increase in interplanar distance (d spacing) is mainly due to the (-OH) containing functional groups in between the graphene layers. After treating with hydrazine hydrate crystalline peaks disappear and a broad peak appears between 18° to 30°. The interlayer spacing increases to 3.5 Å which indicates that the oxygen and water removal takes place and the layer was formed to a large extent. The peak at $2\theta \approx 25.8$˚corresponds to formation of graphene by reduction of graphene oxide under both hydrazine and thermal annealing treatment.

To confirm the formation of graphene further Raman study was performed to support XRD pattern analysis. The spectra consist of three prominent characteristic peaks, namely the D band, the G band, and the G (or 2D) band. The Raman spectroscopy as shown in Figure 5.3a of graphene shows G mode appearing at 1582 cm^{-1}, the other Raman modes are seen at 1350 cm^{-1} (D mode), 2694 cm^{-1} (2D mode), 2964 cm^{-1} (D+G mode) and 3147 cm^{-1} (2D' mode). A few less intense peaks called the D, D+G, D+D, G+D, 2D etc. are also observed. The I(D):I(G) was calculated as 1.24.

The FTIR spectra of Graphene oxide and Graphene are shown in Figure 5.3b. The double peak at 2924 cm^{-1} and 2664 cm^{-1} corresponds to symmetric and unsymmetrical stretching vibrations of ($-CH_2$). Graphene oxide mainly consists of oxygen containing functional groups in

large number, eventually it hampers the conducting property of the sample and mainly behaves like an insulator.

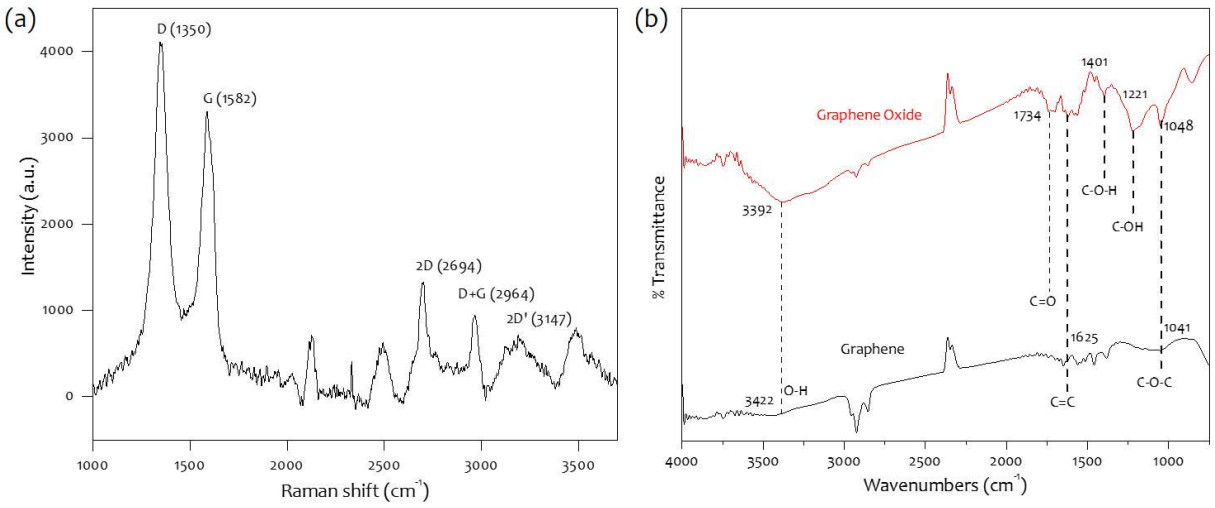

Figure 5.3 : (a) Raman analysis of graphene and (b) FTIR analysis of graphene oxide and graphene

The characteristic band at 1048, 1221, 1401, 1625 and 1734 cm^{-1} peaks corresponds to (C-O-C) stretching vibrations, the (C-OH) stretching peaks, the (–O-H) deformation of the (C-OH) group, the (C=C) stretching and (C=O) stretching vibrations of (–COOH) groups, respectively. The broad peak at 3392 cm^{-1} represent the absorption of water. In graphene, the functional groups of (C-OH) and (–COOH) have disappeared. This indicates that the reduction of graphene to graphene was successfully performed.

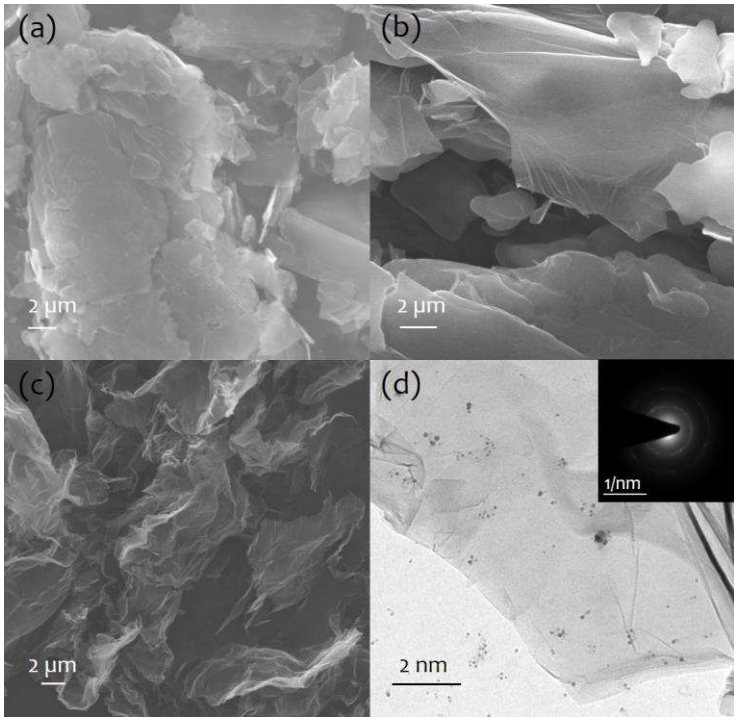

Figure 5.4 : SEM images of (a) graphite, (b) graphene oxide, (c) graphene and (d) TEM image of graphene

The work function of synthesized graphene was recorded to be 4.7eV. The electron microscopy images of synthesized graphene is shown in (Figure 5.4a). The extent of the reduction process was observed from the Figures 5.4a, b and c the, first graphite was reduced to graphene oxide and then again it reduced to graphene. The same Figure 5.4 reveals the nature

of graphene sheets along the process. The single layer graphene sheets appear to be uniformly reduced. During the reduction, removal of oxygen and water from graphene oxide was the main reason behind the separation between the graphitic layers and appearance of fluffy morphology of graphene. TEM image was able to clear surface morphology of graphene (Figure 5.4d). Large number of wrinkles were observed on the graphene sheets which could indicate the presence of various functional groups like epoxy. The presence of droplets on the graphene sheet was caused by the sample preparation during TEM imagining.

5.1.3 Stability and performance study of counter electrode

This study proposes an efficient method for fabrication of graphene counter electrode in dye sensitized solar cells. In working principle of DSSC, the dye molecules were excited due to photon absorption and then the excited dye molecule, injects electron in the conduction band of TiO_2. The dye goes to its original state by getting electron from the redox electrolyte system. Electron transfers to the counter electrode via load. Then electrolyte system was regenerated by the reduction of triiodide at the counter electrode. The counter electrode has two main roles, charge transport and catalyzing the electrolyte system. Likewise, the specific surface areas, high conductivity, the adhesion between the counter-electrode layer and the FTO substrate and the work function of catalyst (graphene) exert their influence on the solar cells photo-conversion performance [Wang, *et al.*, 2008].

Three different methods have been explored to prepare graphene electrode. The XRD patterns of graphene films prepared by different processes are shown in Figure 5.5. Among all, screen printing technique was able to be persistent with standard graphene peak at $2\theta \approx 25.8°$ (see Figure 5.5c). The 400°C was appeared as best annealing temperature compared to other. However, the other two approaches were not able to maintain desired characteristics peak of synthesized graphene films. The peaks observed through these two approaches has been observed at around $2\theta \approx 15^{\circ}$ which is very near to graphene oxide peak as shown in Figure 5.5a and b. The presence of nafion and ethanol at the time of solution preparation would be responsible for the peak shifted towards graphene oxide peak.

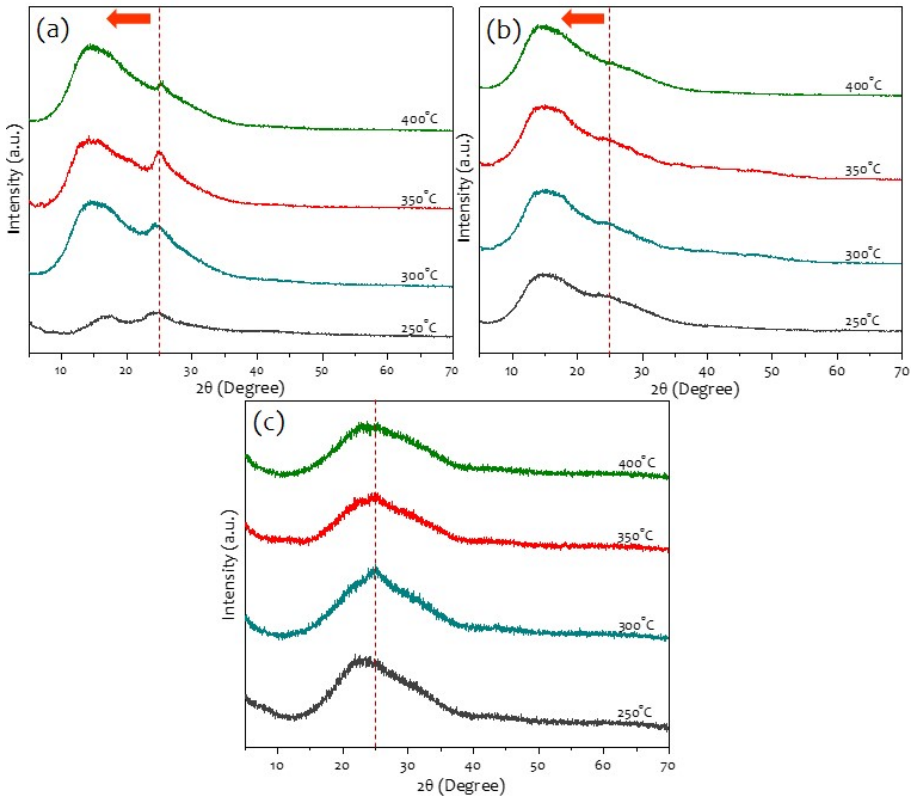

Figure 5.5 : XRD patterns of film surface fabricated at various temp by (a) drop casting, (b) spin coating and (c) screen printing respectively. Dotted line is a eye guide to understand graphene peak

The SEM analysis was performed to reveal the nature of films shown in Figure 5.6, the film prepared by drop casting and spin coating methods showed randomly agglomerated graphene sheets all over the films (see Figure 5.6a and b). The film prepared by screen printing process reveals excellent uniformity (Figure 5.6c). Screen printing technique showed prominent adhesion between the counter electrode film and glass (FTO) substrate with few micron uniform thick film. The agglomeration of nanoparticles during fabrication was the main reason behind nonuniform film formation by the other two techniques. However, to avoid agglomeration of graphene sheets, molecule such as polymers must be used as a host material. So, PEG in screen printing solution act as host molecule to the graphene sheets, no agglomeration of graphene sheets in the film formed by screen printing technique was observed.

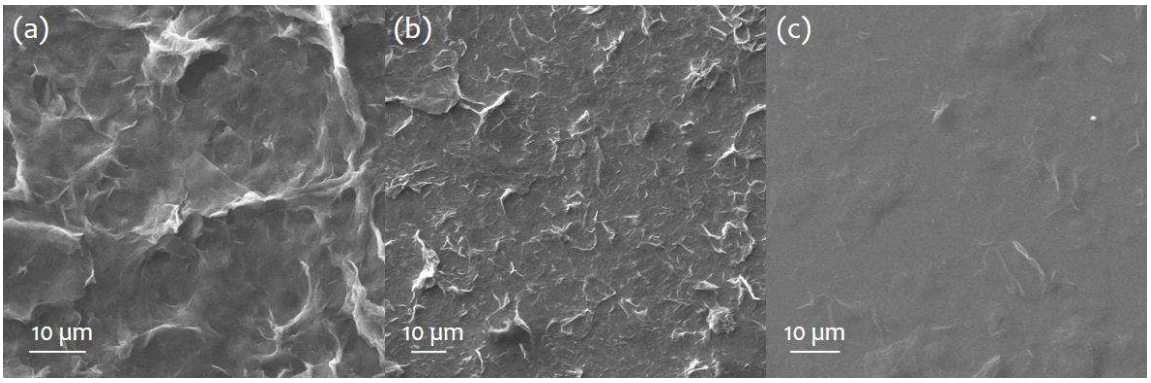

Figure 5.6 : SEM images of film surface fabricated by (a) drop casting, (b) spin coating and (c) screen printing respectively

A photograph of one of the DSSC is shown in Figure 5.7a and inset illustrates the schematic representation of graphene counter electrode DSSC. The current density-voltage curve of all DSSCs are reported in Figure 5.7b.

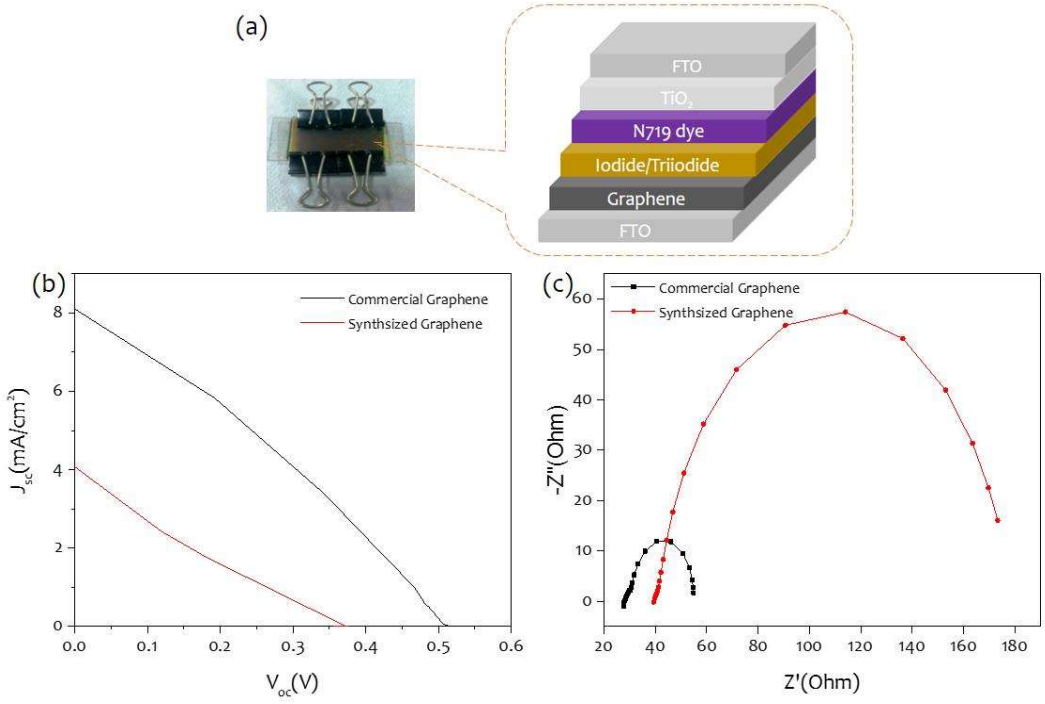

Figure 5.7 : (a) Photograph of graphene counter electrode DSSC with its schematic representation (b) current density-voltage curve and (c) Impedance study of all DSSCs

It has been observed that the synthesize graphene as a counter electrode under one sun showed 0.37 V open circuit voltage (V_{oc}) and 4.1 mA/cm^2 as short-circuit current density (J_{sc}). For comparison, commercial graphene counter electrode DSSC was fabricated, the same procedure was followed to fabricated DSSC. The commercial based counter electrode solar cell has exhibited more V_{oc}, 0.5 V and J_{sc}, 8.1 mA/cm^2. The impedance study was performed to support these photovoltaic characteristics (Figure 5.7c). The performance of the DSSC with synthesized graphene was about 50% less than the DSSC with commercial graphene. It might be due to the fact that functional groups has been not fully reduced during conversion of graphene oxide to graphene. Graphene was synthesized from graphite using sodium nitrate, potassium permanganate and concentrated sulfuric acid. Firstly, graphene oxide was synthesized where it has been reported by the presence of various functional groups like hydroxyl, carboxyl and epoxy. These groups make graphene oxide to act as an insulator, so that is the main reason why graphene oxide was not suitable candidate as counter electrode in DSSC. Then synthesized graphene oxide was converted to graphene by a simple reduction process involving exposure of graphene oxide to hydrazine hydrates. But when graphene is synthesized by this method even after reduction, graphene shows hydroxyl and epoxy groups on sheets and carboxyl groups at the edges, which results in the loss of pristine graphene properties.

This also leads to the observation that the chemical method which includes reduction of graphene oxide not able to prepare pure graphene and synthesized graphene still contains sp^3 groups which were confirmed by Raman spectroscopy. The presence of such functional groups in graphene affects the electrical and physical property of graphene. This would also affect the performance of the DSSC. The commercial graphene prepared by physical route were more suitable than the graphene synthesized from of graphene oxide by chemical method as counter electrode in DSSC.

5.2 CARBON COATED STAINLESS STEEL AS COUNTER ELECTRODE FOR DSSC

One of the carbon allotropes, 2-D graphene, has emerged as an interesting material for counter electrodes material, shows a single layer structure of graphite. The structure of graphene corresponds to well separated 2-D graphite sheets composed of sp^2 bonded carbon atoms arranged in hexagonal structure. It has attracted much attention of researchers to use carbon-based materials for carbon electrodes because of their good chemical stability, low cost, catalytic activity and high conductivity. These carbon materials graphene, CNTs, activated carbon, metal loaded carbon, carbon powder, shows capability to substitute traditional platinum-based counter electrode [Tao, *et al.*, 2015; Bonaccorso, *et al.*, 2010; Han, *et al.*, 2010].

The DSSC mainly consists of photoanode, electrolyte and counter electrode. Traditionally, the counter electrode widely used in DSSC is made of platinum coated conducting glass substrates, where they act as catalyst and charge transporter. Platinum counter electrode has a better performance however it implies 60% of the total DSSC fabrication cost [Kim, *et al.*, 2012]. However, glass substrate shows limitations respect to shape and fragileness. To reduce the cost of the DSSC and broaden their applications in large scale, it is necessary to develop new counter electrode based on other substrates like metal substrates.

Despite having good potential to replace glass substrate form counter electrode, metal substrates like copper, nickel, and aluminum has corrosion stability issue with electrolyte. Metal sheets, stainless steel, have low sheet resistance, excellent electrical and thermal conductivities, and are low in cost. It is anticipated that the application of a metal substrate as a cell electrode substrate can not only reduce the fabrication cost of the DSSC, but also provide better performance of the solar cell by reducing the internal resistance and it also opens a big window for flexible DSSC.

5.2.1 SS-Carbon material DSSC

In this study, a new type of counter electrode for dye sensitized solar cells has been fabricated using a stainless-steel sheet as substrate and graphite, graphene and multiwall carbon nanotubes as the catalytic material, where screen printing technique was opted to

fabricate electrodes. The sheet resistances of SS-graphite, SS-graphene SS-MWCNT and SS-platinum and their influence as counter electrode on the dye sensitized solar cells has been studied.

All DSSCs were fabricated with different counter electrodes were made up of natural graphite powder, graphene (Industrial quality grade G01, Reinete), and MWCNT (Sigma-Aldrich). Instead of FTO, stainless steel was used as a substrate in the counter electrode. Stainless steel sheet (grade 304) was cleaned by detergent, distilled water and acetone respectively for 10 minutes each by and then dried into vacuum furnace at 50˚C for 10 minutes.

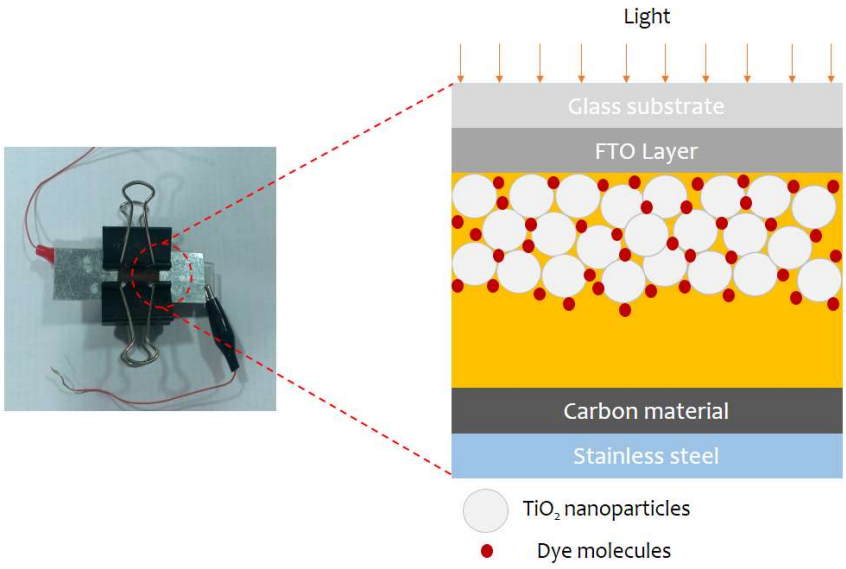

Figure 5.8 : Photograph of SS-catalyst counter electrode DSSC and inset shows a schematic illustration of DSSC where carbon materials are graphite, graphene and MWCNT

The composite paste of carbon materials was prepared for screen printing to fabricate counter electrodes. In short, natural graphite powder, ethyl cellulose as a binder and terpineol as a surfactant were stirred together for 24 hours. The same procedure was followed to prepare graphene and MWCNT pastes. These pastes has been used for growing films on SS by screen printing technique. Also, platinized SS counter electrode was fabricated by brush painting technique using platisol as a precursor. All SS substrate counter electrodes were annealed at 380˚C for 12 hours in air atmosphere. The photoanode and DSSC fabrication were prepared by following exact same process mentioned in the Annexure A: Materials and methods.

5.2.2 Structural, electrical and J-V performance of SS-Carbon material DSSC

The Figure 5.8 shows photograph of SS-catalyst counter electrode DSSC and inset represents a schematic illustration of DSSC. To study surface morphologies and the role in cell performance, scanning electron microscope imaging (SEM) were performed. The Figure 5.9 shows the surface morphology of SS-graphite, SS-graphene, SS-MWCNT and SS-platinum counter electrodes. All ~ 11 micron thick SS-carbon material counter electrodes has been prepared screen printing technique as described in the previous section. Usually, in screen printing technique poly ethylene glycol or ethyl cellulose is added during preparation of screen printing paste. As discussed previously, these polymers act as a host material to form a uniform film. Despite adding polymers in the screen printing pastes, graphite, graphene and MWCNT films has been reported presence of the agglomerated carbon catalysis materials on the film surface (see Figure 5.9a, b and c respectively). These agglomerations have direct impact on cell efficiency as it hinders the electron transfer pathway which eventually increases the resistance. This might be the reason behind low conversion efficiencies of DSSCs. However, platinum counter electrode was prepared by platisol by brush coating tends to form uniform film as seen in Figure 5.9d.

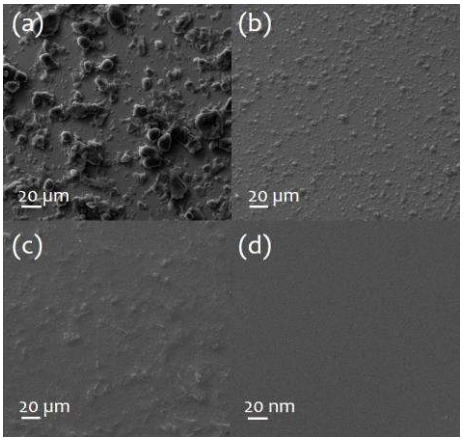

Figure 5.9 : Shows the SEM photographs of the SS coated with (a) graphite, (b) graphene, (c) MWCNT and (d) Pt

The sheets resistance (R_{sh}) has direct influence on the performance of the DSSC, it increases the resistance in the cell. From Table 5.1, it has been observed that after platinum coating no significant change was reported in the sheet resistance of the SS. Whereas, on the other hand the sheet resistances of the SS coated with graphite (SS-graphite) were reported with remarkable increment. In the other two cases, SS coated with graphene (SS-graphene) and MWCNT (SS-MWCNT) were appeared with increment in the sheet resistance, where among all carbon materials SS-graphene was shown less increment in sheet resistance.

Table 5.1: Properties of SS with different counter electrodes

Catalytic materials	*R_{sh} of blank SS Substrate (Ω/sq)*	*R_{sh} of SS-catalytic material (Ω/sq)*
Graphite	0.23	1.32
MWCNT	0.21	1.08
Graphene	0.21	1.02
Platinum	1.02	0.22

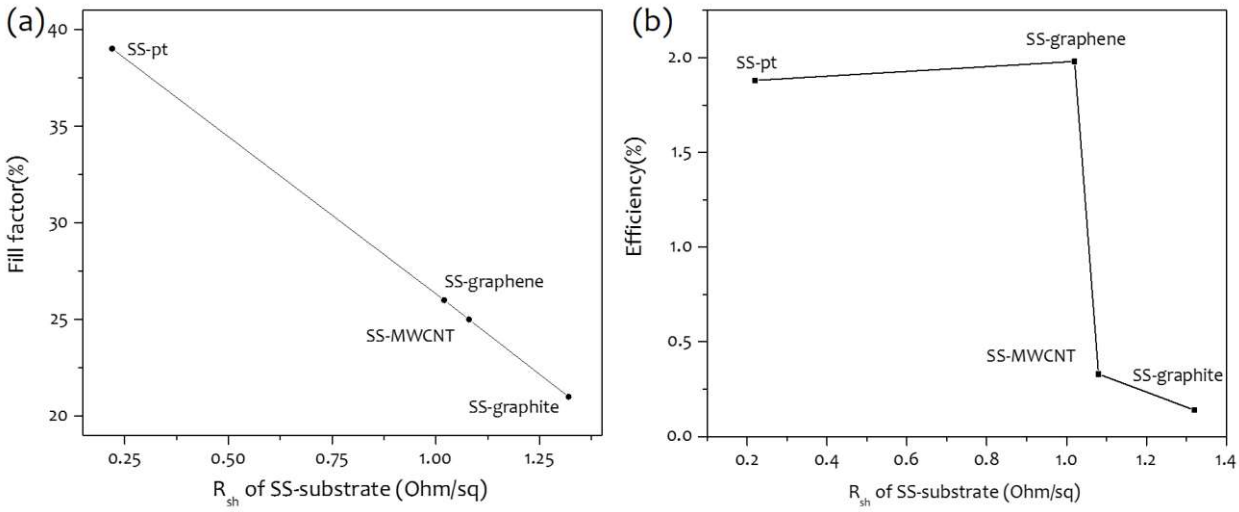

Figure 5.10 : Relation between the (a) R_{sh} of various SS-substrates and fill factor, and (b) with DSSC efficiency

A low sheet resistance of the electrode substrate is one of the key factors behind high performing DSSC. The series resistance of the DSSC is mainly considered to consist of the sheet resistance of the electrode substrate and the resistance created by the porous TiO_2 electrode and

electrolyte, therefore sheet resistance could directly influence the fill factor and efficiency of the DSSC. The correlation between sheet resistance and different parameters of DSSC were demonstrated in the Figure 5.10.

The fill factor and efficiency of the solar cells are the key parameters which derives the solar cell photoconversion performance (see Figure 5.10a and b). This study reveals that the sheet resistance of SS-substrates has been increased from 0.22 to 1.32 ohm/sq and directly leads to lower the fill factor from 39% to 12%.

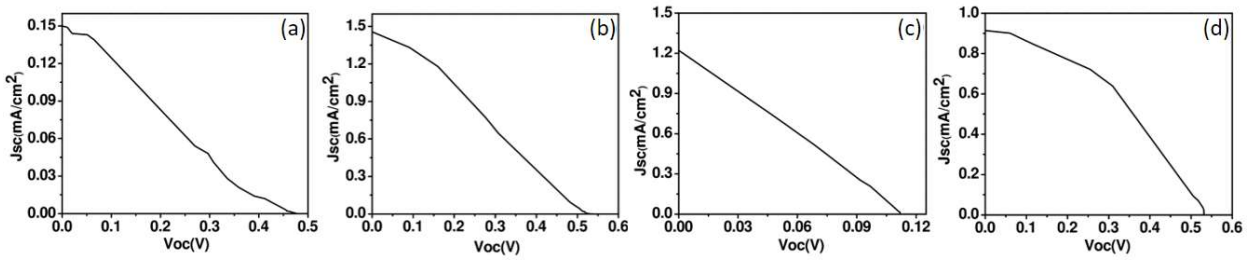

Figure 5.11 : Shows the SEM photographs of the SS coated with (a) graphite, (b) graphene, (c) MWCNT and (d) Pt

Despite the SS-graphene were able to show more sheet resistance compare to SS-Pt, SS-graphene counter electrode DSSC recorded high efficiency 1.98% compared to SS-Pt counter electrode DSSC.

The photovoltaic performances of all DSSCs, SS-graphite, SS-graphene, SS-MWCNT and SS-Pt counter electrode are shown in Figure 5.11 and all DSSC parameters are summarized in Table 5.2. All cell has been analyzed under standard one sun radiation. The DSSCs with a SS-graphene counter electrode has a reported 1.98% efficiency which is highest efficiency among all, whereas that of a SS-graphite counter electrode is only 0.14% (see Figure 5.11b and a respectively). The enhanced performance has been supported the SS as substrate at counter electrode with carbon material-catalyst. Carbon material, graphene have been reported with remarkable good conductivity and catalytic activity [Wang, *et al.*, 2007]. With metal substrate in counter electrode, low sheet resistance of stainless steel enhanced the electron transfers pathway or resistance, 2D material like graphene could shorten the pathway than that in 1D MWCNT, favors the charge-transfer accessibility with minimum possibility of charge scattering. These are the main reasons to show high photo conversion efficiency at SS-graphene counter electrode DSSC compared to other cells.

Table 5.2: Comparison of SS-carbon material DSSC photovoltaic performance

Electrode materials	J_{sc} *(mA cm^{-2})*	V_{oc} *(V)*	*FF (%)*	*η (%)*
Graphite	0.l5	0.47	21	0.14
MWCNT	1.46	0.524	26	1.98
Graphene	1.22	0.11	25	0.33
Platinum	0.91	0.53	39	1.88

The redox reduction rate at counter electrode is one of the crucial factors in operation of the DSSC and have direct impact on cell performance. The redox reaction mostly takes place at electrolyte/counter electrode and electrolyte/dye molecule on photoanode interfaces. At the surface of the counter electrode, firstly electrolyte transports the positive charges specifies to counter electrode and couple redox is then reduced, simultaneously couple redox reduces the oxidized dye to regenerate the dye molecules. To function DSSC efficiently, the redox reaction in electrolyte becomes more important to transport charge from photoanode and counter electrode. But previous studies have always encountered with stability issues and corrosion of metal substrate. On the other hand, triiodide is strong oxidant and it rapidly age the SS. In the

process of ionic diffusion, catalytic redox species, charge transfer at counter electode and electrolyte together could trigger the process of corrosion.

5.3 GRAPHENE COUNTER ELECTRODE WITH SUB-ZERO TEMPERATURE, ZnO-TiO_2 AND H-HfO_2/TiO_2 NANOSPHERES AS PHOTOANODE MATERIALS

5.3.1 Effect of working area on DSSC performance

The working area of photoanode have direct influence on all the DSSC parameters, J_{sc}, V_{oc}, FF and η [Vendra, *et al.*, 2012; Fakharuddin, *et al.*, 2013]. Limited work has been reported on this, where researchers have investigated and formed a correlation between working area and electron lifetime, resistance and path length. Even few study have reported observations where working area effect on cell performance was investigated by using kinetics of electron-hole recombination. In this study, the effect of working area on DSSC performance was demonstrated.

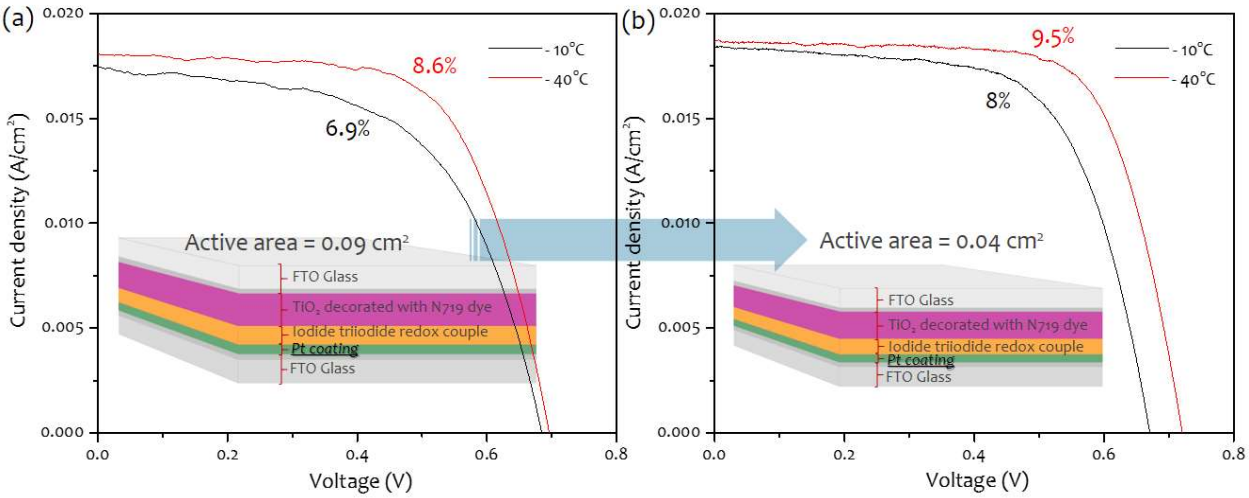

Figure 5.12 : Current density – voltage curves of the DSSC consisting -40 °C and -10 °C samples as photoanodes with (a) 0.09 and (b) 0.04 cm^2 active area respectively, under one sun illumination

To study the working area effect, DSSCs with TiO_2 synthesized at subzero temperatures at -40°C and -10°C were fabricated according to the process described in the Annexure A: Materials and methods. As discussed in chapter 3, the DSSC with -40°C as photoanode have reported very small particle size, high specific surface area and anatase dominating TiO_2, and shown high efficiency of 8.6% (see Figure 5.12a). As discussed before at -10°C, particles were formed in nanorods shape and exhibited high weight percentage of the rutile phase, less lattice strain and low defects compare to other TiO_2, and reported with 6.9% efficiency as shown in Figure 5.12a. The working area of these cells were preciously kept constant at 0.09 cm^2 using screen printing mesh size. There were few reports which emphasized on the decreasing active area of photoanode and reported with remarkable photocurrent density with enhanced photo-conversion efficiency of the DSSC [Fakharuddin, *et al.*, 2013]. The same fabrication process was followed to prepare all DSSCs but to understand the working area effect, the cell area has been reduced to 0.04 cm^2.

The photovoltaic performance of TiO_2 synthesized at subzero temperatures (-40 and -10°C) photoanode DSSCs are shown in the Figure 5.12. In the same Figure, inset shows schematic representation of prepared DSSCs. As it can be observed, all photovoltaic parameters, J_{sc}, V_{oc}, FF and η were increased on decreasing active area from 0.09 to 0.04 cm^2. At 0.04 cm^2 active area, the -40°C cell shows the highest J_{sc} up to 18.46 mA/cm^2 compared to 18.46 mA/cm^2 for 0.09 cm^2 active area cells (see Figure 5.12a and b respectively). At -40°C, the increase in photoconversion efficiency is lower (Δη ~ 11%) than the -10°C (Δη ~ 15%), however, these increments in efficiency show its correlation with the active area.

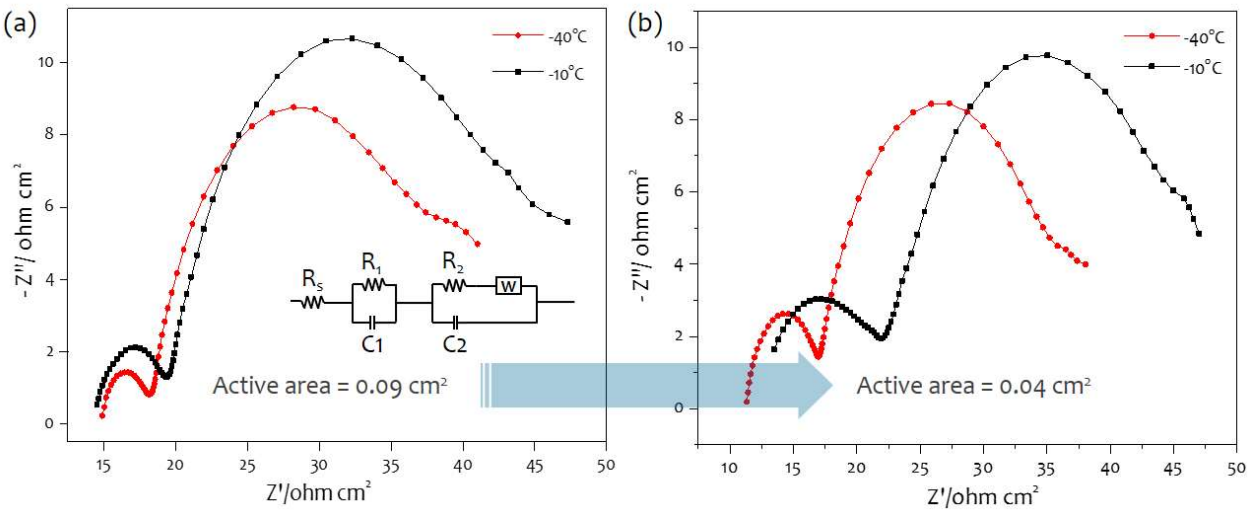

Figure 5.13 : Nyquist plot of -40 °C and -10 °C samples DSSC with (a) 0.09 and (b) 0.04 cm² active area respectively

The impedance study, Nyquist plots of different active area DSSCs of -40 and -10°C were shown in Figure 5.13 and inset illustrate the equivalent circuit. Every plot consists of three semicircles. The first semicircle corresponds to the charge transport along Pt-electrolyte interface the middle represents transfer at TiO_2-electrolyte-dye interface, and the third semicircle indicates the redox species diffusion across the system. The size of these semicircles has been reduced with decreased active area of photoanode (see Figure 5.13a and b). The values of R_s, R_1 and R_2 were reduced as the size of these semicircles. This can be explained by the inverse relationship between resistance and active area [Shin, *et al.*, 2010]. The R_s, resistance at electrodes was independent of active area, it has been reported in previous study that working area is significantly big then the R_s also have cumulative effect on the total resistance produced during charge transport. Other resistance R_1 and R_2 has been decreased with decreasing active area from 0.09 to 0.04 cm², this reduced the transfer path and facilitated more charge transport with less recombination, eventually harvested more photon. So, as the active area of photoanode decreases it directly increases the photo-conversion efficiency of DSSC.

5.3.2 Titania at sub-zero temperature, ZnO-TiO_2 and H-HfO_2/TiO_2 nanospheres as photoanode materials

As disused in chapter 5, graphene material has good potential to replace traditional Pt counter electrode from the DSSC. The cells were fabricated with 0.04 cm² active area and consist of TiO_2 synthesized at subzero temperatures at -40°C and -10°C, where detail fabrication process described in the Annexure A: Materials and methods. In these DSSCs graphene-FTO (catalyst-substrate) as counter electrode have been used. Photoanode thickness was observed to be of ~15 µm. The current density-voltage (J-V) curves of DSSC devices having Pt and graphene counter electrodes are shown in Figure 5.14a and b respectively. The performance of the -40°C solar cells was reduced by $\Delta\eta$ ~ 10% on replacing Pt counter electrode with graphene. The highest photo conversion efficiency (9.6%) has been reported with Pt counter electrode, whereas same composition with graphene counter electrode shows 8.6% efficiency. Graphene, 2d sheets of sp^2 bonded carbon atoms have high conductivity, good chemical stability and most importantly it showed significant catalytic activity but still it not able to beat the Pt electrode performance. The same trend was observed with -10°C solar cells where efficiency was reduced by 5% (see Figure 5.14).

The best performing 1% ZnO-TiO_2 and H-HFO_2/TiO_2 were used for further analysis with graphene counter electrode as shown in Figure 5.15a and b respectively.

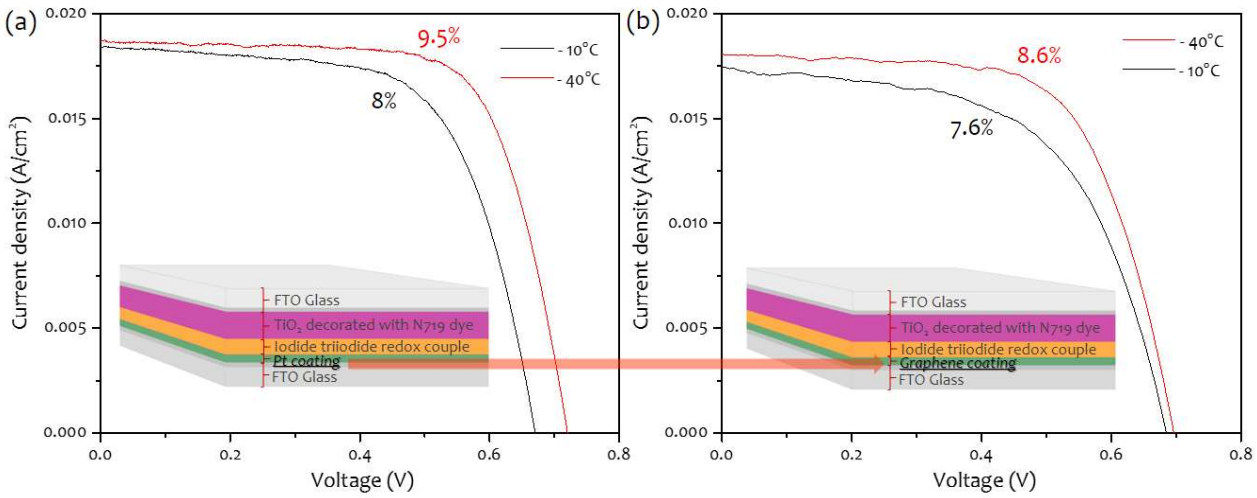

Figure 5.14 : Current density – voltage curves of the DSSC consisting -40 °C and -10 °C samples as photoanodes with a) Pt and b) graphene counter electrode with 0.04 cm^2 active area

With graphene counter electrode, 1% ZnO-TiO_2 DSSC have been reported with decrease in efficiency by 10% (see Figure 5.14a) and photocurrent density was reduced from 18.96 to 17.42 mA/cm^2. The same observations were observed with H-HFO_2/TiO_2 photoanode, with Pt counter electrode high photocurrent density (21.74 mA/cm^2) has been observed. However, graphene counter electrode reduced this value to 17.88 mA/cm^2 and resulted in lesser efficiency ($\Delta\eta \sim 10\%$).

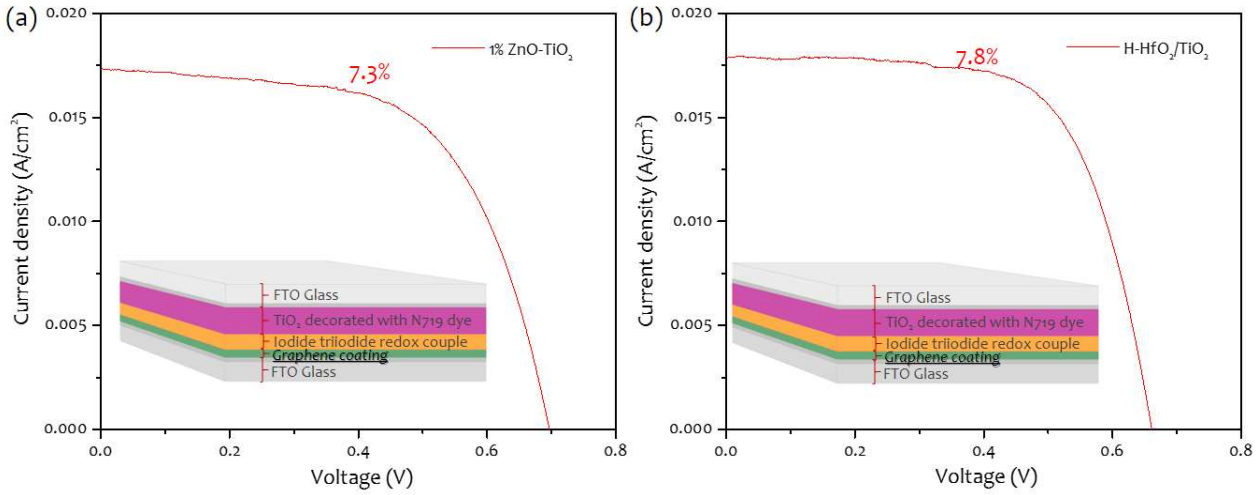

Figure 5.15 : Current density – voltage curves of the DSSC consisting (a) 1% ZnO-TiO_2 and (b) H-HfO_2/TiO_2 samples as photoanodes with graphene counter electrode with 0.04 cm^2 active area

The traditional counter electrode has better performance but it implies about 60% of the total fabrication cost. So, replacement of Pt with graphene in counter electrode of DSSC is viable even graphene has been reported with less efficiency.

5.4 CONCLUDING REMARKS

This study shows synthesized graphene have a good potential to replace traditional Pt counter electrode in DSSC. With optimized annealing temperature screen printed FTO glass substrate was proven to be a promising candidate for counter electrode. This work also throws light on how the process adopted in making graphene plays a key role in determining the catalytic behavior of the synthesized graphene as counter electrode. Among the various carbon

materials based counter electrode with stainless steel as a substrate graphene shown the best performance. This study also exhibits the correlation between working area of photoanode and photoconversion efficiency of the cell. On reducing working area, remarkable photocurrent density enhanced the photoconversion efficiency, which is due to increased electron lifetime, path length with less resistance.